

A Perspective Analysis on the Effects of Additives on the Microstructure and Mechanical Properties of AlSi10Mg

Dr G Raja Kumar ¹, Perumallapalli Gandhi ², Dr. B. Ravi ³

Assistant Professor ^{1,2,3}

Department of Mechanical engineering,

^{1,3} Swarna Bharati Institute of Science and Technology, Khammam, TS-507002

² SV engineering college, Surya Peta (DIST). TS-508213

ABSTRACT:

In the field of Additive Manufacturing (AM), selective laser melting (SLM) outperforms layer-by-layer melting for the production of complicated and one-of-a-kind components. This effort is focused on improving the SLM technique so that high-density AlSi10Mg alloy components may be manufactured. To check for microstructural issues and macrostructural problems, the AM specimens were analysed using optical microscopy and scanning electron microscopy (SEM), respectively. Also investigated were the effects of layer thickness on two mechanical properties of AlSi10Mg alloy components: microhardness and ultimate tensile strength (UTS). Based on the results, the microstructure of the deposited layer displays distinct patterns and behaviours both at the melt pool's border and farther into the layer. As the layer thickness decreased, the tensile strength increased, going from 60 m to 30 m. The enhanced surface form, reduced porosity, and ultra-fine cellular dendritic microstructure are likely to blame for this. Horizontal tests showed that samples with a 30 m layer thickness had a 24% higher UTS than those with a 60 m layer thickness.

Keywords: density, layer thickness, UTS, microstructures, AlSi10Mg, SLM, and ultrathin films;

I. INTRODUCTION

Parts with complicated geometries and a requirement for lightweight, strong materials have made SLM one of the most promising technologies in recent years, especially in the aerospace and medical industries [1-3]. Additive manufacturing is a method that generates 3D objects via layer-by-layer production and joining, as opposed to traditional manufacturing procedures. This process begins with the application of a coating of metal powder, which is then melted and quickly solidified by irradiating it with a laser. When the laser interacts with the substance, the exposure time will be only a few milliseconds. As a result, AM is thought of as a high laser power-density method with a reduced contact time [5-8]. Because of its high reflectivity and excellent thermal conductivity, AM of Al alloy powders presents a few difficulties. Consequently, the amount of laser power needed to melt Al alloy powder was greatly increased. In addition, Al alloys are prone to porosity production, which is caused by the oxidation of oxide inclusions and leaves weak places in the AM that are created. Rapid melting and solidification play a crucial role in the SLM process. These factors impact the material's mechanical characteristics and should be thoroughly studied. The SLM process may be used to create components with a controlled texture and an exceptionally fine microstructure of AlSi10Mg, according to Kempen k [4,8]. The purpose of this study is to investigate the effects of additive manufacturing on the microstructure, hardness, and tensile strength of an AlSi10Mg alloy. The research will compare the findings to existing literature to determine if the alloy can achieve

the same or similar properties through heat treatments, surface coating, platform temperature, and variation in process parameters, with two different layer thicknesses of 60 μ m and 30 μ m, respectively, while reducing production time and costs.

II. EXPERIMENTAL METHODS

The studies were conducted utilising a powder-bed AM machine that specialises in selective laser melting (Model: SLM 280HL). Commercially available AlSi10Mg aluminium alloy powder was used in the research. In Table 1 we can see the chemical make-up of the AlSi10Mg alloy powder that was used for this investigation. The size distribution of the particles ranged from 20 to 70 μ m. A Ytterbium fibre laser with a maximum power of 400 W and a spot size of 80 μ m (dia) is attached to the SLM 280HL system. In this investigation, we scanned at a speed of 500–700 mm/s using a laser power range of 170–250 W. In order to examine how the microstructure and mechanical properties of the AlSi10Mg alloy components produced by AM were influenced by the layer thickness, this research used two distinct thicknesses, 30 μ m and 60 μ m. Argon gas was used to safeguard the melt pool during SLM trials. A continuous flow rate of Argon was used to keep the oxygen level below 200 ppm throughout the SLM trials. Figure 1 is a schematic representation of the SLM procedure.

Optical microscopy and high-magnification scanning electron microscopy were used to examine the microstructure and macro characteristics of the AM-built components. Following the conventional metallography process, samples were polished and etched after being transversely sliced 3 mm below the building's top. Chemical etching was performed on the specimens using the keller's reagent solution.

TABLE I. CHEMICAL COMPOSITION OF ALSI10MG POWDER

Al	Si	Fe	Cu	Mn	Mg	Zn	Ti
Balance	9.0-11.0	0.3	0.03	0.001-0.4	0.2-0.5	0.1	0.15

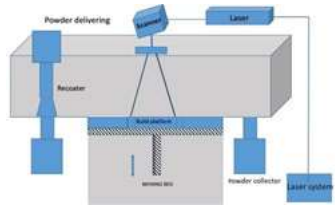


Figure 1. Schematic diagram of SLM

Hardness of the parts were accessed by utilizing a Micro- Vickers hardness tester with an applied load of 100 g and a dwell time of 10 sec. An average of indentations was taken. Further, uniaxial tensile testing was carried out with a cross- head speed of 1 mm/min. Total three tensile test specimens were accessed in each condition and the specimens were prepared based on the ASTM E8 standard.

III. RESULTS AND DISCUSSION

A. Powder Charectaristics

Powder flowability and melting behaviour are both affected by the particle size distribution, which is well known. Figure 2(a) shows a scanning electron micrograph of AlSi10Mg powder. Particle sizes in the powder are shown in Fig. 2(b), ranging from 21 μ m to 69 μ m. The shape of the AlSi10Mg powder is described as very irregular and complicated. It is also clear that the big powder particles were linked to the smaller, less regular particles.

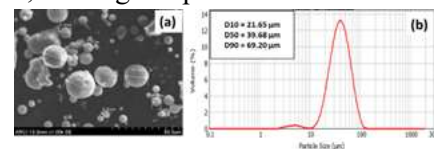


Figure 2. (a) SEM images, and (b) Particle size distribution of AlSi10Mg powder

Also, certain powder particles consist of fine internal pores which was originated during atomization process by entrapment of gases. These can significantly influence the quality of the AM built part by forming the gas pores in the AM built during solidification.

B. Microstructural Analysis of AlSi10Mg AM built specimens

SLM process being a layer by layer melting with fast and directional cooling sequence creates an extremely fine and unique microstructures in the AM built components.

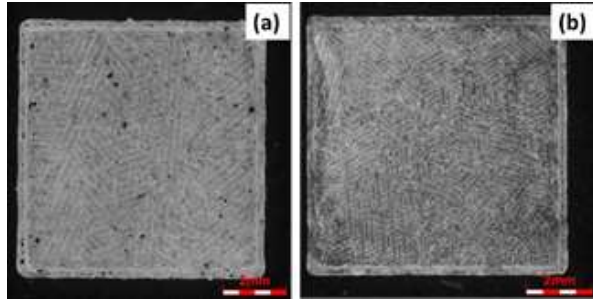


Figure 3. Top view of micro structure of AM built AlSi10Mg (a) 60 μm (b) 30 μm

Fig 3(a) and (b) depicts the micrographs of the top section of AM built AlSi10Mg specimen built in the horizontal direction with a layer thickness of 60 μm and 30 μm. The porosity distribution in cross-section exhibits the top view of the AM built melt pool.

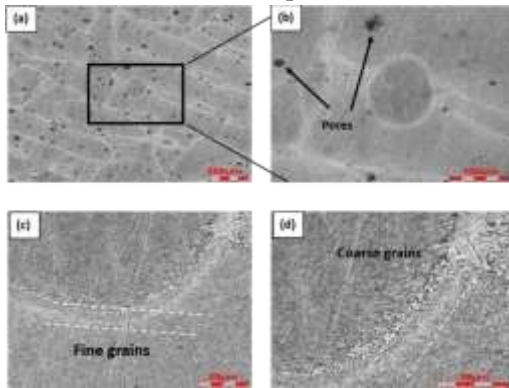


Figure 4. Optical images of AlSi10Mg @ 60 μm layer thickness (a) microstructure @ 200X (b) Microstructure @ 693X magnification and (c) Microstructure @ 2000X magnification (d) microstructure @ 4000X

The microstructure was characterized by a fine dendritic microstructure Figs. 4 and 5 formed due to rapid cooling. The morphologies of the cells are different as the build layer size changes. The microstructural features of the specimens were examined and the porosity in the AM built samples with a layer thickness of 60 μm is higher

than the samples with a layer thickness of 30 μm. It shows that the scanning direction of each layer is typically different characteristics.

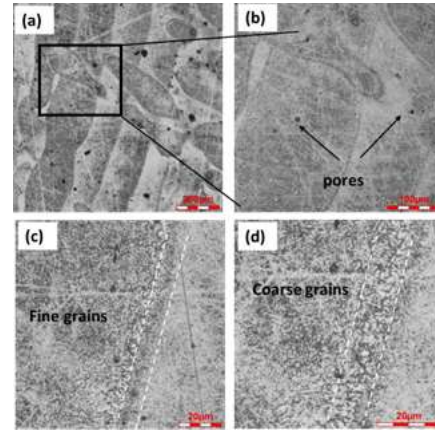


Figure 5. Optical images of AlSi10Mg @ 30 μm layer thickness (a) Macrograph (b) Microstructure @ 200X magnification and (c) Microstructure @ 6393X magnification (d) @ 2700X magnification (e) @ 4000X magnification

C. Mechanical properties of AM built Samples

Fig. 6 shows the tensile stress-strain curves for the AM built AlSi10Mg specimens produced with different layer thicknesses and the tensile test results are tabulated in Table

2. It has been observed that the horizontal built samples exhibit better Tensile Strength than the vertical build samples. Therefore, it can be inferred that the unique distinguishing factor for improvement in the tensile properties was sample orientation and layer thicknesses.

TABLE II. TENSILE TEST RESULTS

Specimen	Y.S (MPa)	U.T.S (MPa)	% Elong.
60μm-H	232	359	7.81
60μm-V	236	340	4.43
30μm-H	265	446	9.63
30μm-V	268	469	8.18

Results show the variation in YS and UTS between the vertical and horizontal built samples. And the UTS of 30 μm layer thickness built specimens showed improvement in the

maximum strain at failure as compared to the 60 μm layer thickness specimens.

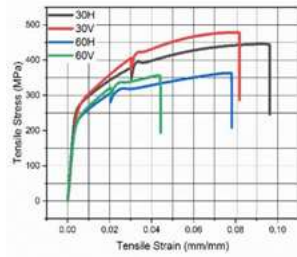


Figure 6: Tensile test results plot different layer thickness and built direction

D. Vertical Build Direction

Table 2 shows the tensile test data, whereas Figure 6 shows the stress-strain graphs of the AlSi10Mg AM that was constructed. The elongation values for AM samples are much greater than the values reported in the literature for cast alloys and T6 treated alloys. The mechanical characteristics of AM samples and cast alloys that have undergone heat treatment are almost identical, with no discernible variation [13, 20]. The absence of these distinctive tiny microstructures in the cast process compared to the AM process is the reason for this improvement.

E. Horizontal Build Direction

Figure 6 shows the stress-strain graphs and Table 2 shows the tensile test data of the AlSi10Mg AM that was constructed. In both the horizontal and vertical planes, the increased elongation stands out as the most notable feature of the AM-built specimens' tensile characteristics. This is because the AM-built specimens naturally took on an anisotropic character as a consequence of the process's directed solidification. The results of this investigation show that the micro hardness of the samples with a 30 μm and 60 μm layer thickness is quite similar. The micro hardness does not rely on the layer thickness in the samples that were additively created.

F. Fracture Analysis of the Tensile Specimen

The fractography method helps us majorly to improve over the process parameters selection and reduction of porosities, which in turn helps us to obtain improved characteristics using the Additive manufacturing process.

The Figs. 7 and 8 shows the magnified view in Scanning Electron Microscope of the fractured surfaces of Tensile tested AM built AlSi10Mg Tensile samples built using the SLM technique. The fractography of the tensile samples shows very rough and irregular surfaces.

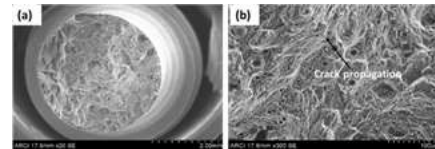


Fig 7. SEM fractography micrographs of 60 μm horizontal built

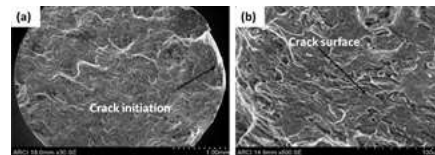


Fig 8. SEM fractography micrographs of 30 μm horizontal built

Fracture morphology presented in the Figs. are characterized by the crack origin and its mode of propagation.

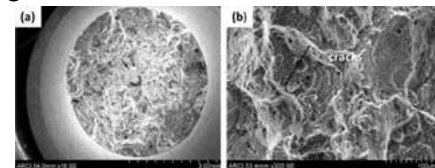


Fig 9. SEM fractography micrographs of 60 μm vertical built

Fracture surfaces with unmelted particles may also be seen at greater magnification. Since the strength may be enhanced by decreasing the layer thickness, images of 30 μm horizontally created samples exhibit a more fibrous texture compared to 60 μm horizontally built samples. Possible influences on the formation of oxide layers, including an increase in porosity and particles that do not melt, include laser power, spot size, and process scanning

speed.

The presence of a dimple in the vertical built at the site of a ductile fracture may be seen in figure 9. (Fig. 9) between layers that are just loosely bound together. Entrapment of argon gas results in the appearance of very fine porosity. Figure 9 shows the absence of unmelted particles and the evident Al—Si fine eutectic cellular structure. Fine dimples and ridges with thick lines may be visible on the horizontal constructed specimen's fracture surface (fig.7). In contrast to the vertically constructed samples, the intricate cellular structure is obscured in this image. The existence of pores, an inevitable and difficult aspect of the AM process, and the anisotropy of the constructed specimens are both seen here. Thus, the horizontally constructed samples exhibit better elongation prior to layer-to-layer fracture compared to the vertically constructed samples. A reason why vertical samples fail sooner than horizontal ones when loosely connected layers are present.

IV. CONCLUSION

- The tensile strength and mechanical characteristics (layer thickness) of the 60µm and 30µm SLM AlSi10Mg samples studied here are comparable, hence it is possible to increase the layer thickness. Although AM technology has the potential to reduce manufacturing costs by shortening build times with increasing layer thickness, this is mostly a drawback of the technology. It was discovered that the two materials with 30 µm and 60 µm layer thickness (124 HV) had roughly comparable Micro Vickers hardness. There is no correlation between the layer thickness and the micro hardness of the AlSi10Mg samples that were produced by additive manufacturing. It has been shown that samples

constructed horizontally exhibit a greater tensile strength compared to ones constructed vertically. Different microstructural features and shapes are seen in the specimens made from AlSi10Mg AM in both the horizontal and vertical dimensions. Superior tensile properties were shown by the specimens with a 30 µm layer thickness compared to those with a 60 µm layer thickness. Possible explanations for this enhancement include a highly refined microstructure, reduced porosity, and an enhanced surface shape.

REFERENCES

1. N, Read; W, Wang; K, Essa.; M, Attallah: Selective laser melting of AlSi10Mg alloy: Process optimization and mechanical properties development, Materials and Design 65, 2015, pp. 417-424.
2. S. Romano, A. Brückner-Foit, A. Brandão, J. Gumpinger, T. Ghidini, S. Beretta: Fatigue properties of AlSi10Mg obtained by additive manufacturing: Defect-based modelling and prediction of fatigue strength, Engineering Fracture Mechanics, 2018, pp. 169-189.
3. E, Brandl; U, Heckenberger; V, Holzinger; D, Buchbinder: Additive manufactured AlSi10Mg samples using selective laser melting (SLM): Microstructure, high cycle fatigue, and fracture behavior. Materials and Design 34, 2012, pp. 159-169.
4. L, Thijs; K, Kempen; J, Kruth; J, Humbeeck: Fine-structured aluminum products with controllable texture by selective laser melting of pre-alloyed

- AlSi10Mg powder. *Acta Materialia* 61, 2013, pp. 1809-1819.
5. J.R. Davis, *Aluminum and Aluminum Alloys*, ASM Handbook, ASM International, Materials Park, 1999
 6. KG, Prashanth; S, Scudino; HJ Klauss; KB, Surreddi; L, Löber; Z, Wang; AK, Chaubey; U, Kühn; J, Eckert: Microstructure and mechanical properties of Al-12Si produced by selective laser melting: Effect of heat treatment. *Materials Science and Engineering A* 590, 2014, pp. 153-160.
 7. NT, Aboulkhair; NM, Everitt; I, Ashcroft; C, Tuck: Reducing porosity in AlSi10Mg parts processed by selective laser melting. *Additive Manufacturing* 1-4, 2014, pp. 77-86.
 8. K, Kempen; L, Thijs; J, Humbeeck; J, Kruth: Mechanical properties of AlSi10Mg produced by selective laser melting. *Physics Procedia* 39, 2012, pp. 439-446.
 9. C A, Biffi; J, Fiocchia; P, Bassania; D S, Paolinob; A, Tridello; G, Chiandussib; M, Rossettob; A, Tuissia: Microstructure and preliminary Fatigue Analysis on AlSi10Mg samples manufactured by SLM ; *Procedia Structural Integrity* Volume 7, 2017, pp. 50-57
 10. J S, Zuback; T, DebRoy; *The Hardness of Additively Manufactured Alloys*, Materials, 2018; pp. 2070.
 11. N, Kaufmann; M, Imran; TM, Wischeropp; C, Emmelmann; S, Siddique; F, Walther: Influence of process parameters on the quality of aluminum alloy EN AW 7075 using selective laser melting (SLM). *Physics Procedia* 83, 2016, pp. 918-926.
 12. H, Zhang; H, Zhu; Qi, T; Hu, Z; X, Zeng: Selective laser melting of high strength Al-Cu-Mg alloys: Processing, microstructure, and mechanical properties. *Materials Science and Engineering: A* 656, 2016, pp. 47-54.
 13. M, Tang; *Inclusions, Porosity, and Fatigue of AlSi10Mg Parts Produced by Selective Laser Melting*; Dissertation, May 2017.
 14. T. S. Srivatsan; T. S. Sudarshan, Eds., *Additive Manufacturing: Innovations, Advances, 147 and Applications*. CRC Press, 2015.
 15. B, Stucker B, Janaki Ram G. Layer-based additive manufacturing technologies. *Materials Processing Handbook*: CRC Press; 2007. p. 1–32.
 16. W.M. Steen, *Laser material processing*, 3rd edn. (Springer, Berlin, 2003), pp. 279–284
 17. M. Gupta and S. Ling, Microstructure and Mechanical Properties of Hypo/Hyper-Eutectic Al-Si Alloys Synthesized Using a Near- Net Shape Forming Technique, *J. Alloys Compd.*, 1999, 287, p 284-294
 18. M. Gupta, C. Lane, and E.J. Lavenia, Microstructure and Properties of Spray Atomized and Deposited Al-7SiSiCp Metal Matrix Composites, *Scr. Metall. Mater.*, 1992, 26, p 825
 19. J. Hatch, *Aluminum: Properties and Physical Metallurgy*, American Society for Metals, Cleveland, 1984
 20. EOS GmbH – Electro Optical Systems. *Material Data Sheet: EOS Aluminium*

AlSi10Mg, www.eos.info, München, 2014.

21. ASTM B85, Standard Specification for Aluminum-Alloy Die Castings, ASTM International, West Conshohocken, PA, 2013
22. ASTM Committee F42, "ISO / ASTM 52900-15: Standard Terminology for Additive Manufacturing Technologies - General Principles - Terminology," ASTM International. ASTM International, 2015.